

This article was downloaded by:

On: 25 January 2011

Access details: Access Details: Free Access

Publisher Taylor & Francis

Informa Ltd Registered in England and Wales Registered Number: 1072954 Registered office: Mortimer House, 37-41 Mortimer Street, London W1T 3JH, UK



Separation Science and Technology

Publication details, including instructions for authors and subscription information:

<http://www.informaworld.com/smpp/title~content=t713708471>

Modeling and Simulation of an Adiabatic Adsorber

P. S. K. Choi^{ab}; L. T. Fan^a; H. H. Hsu^{ac}

^a DEPARTMENT OF CHEMICAL ENGINEERING, KANSAS STATE UNIVERSITY, MANHATTAN,

KANSAS ^b Battelle Memorial Institute, Columbus, Ohio ^c Esso Production Research Company,

Houston, Texas

To cite this Article Choi, P. S. K. , Fan, L. T. and Hsu, H. H.(1975) 'Modeling and Simulation of an Adiabatic Adsorber', Separation Science and Technology, 10: 6, 701 — 721

To link to this Article: DOI: 10.1080/00372367508058051

URL: <http://dx.doi.org/10.1080/00372367508058051>

PLEASE SCROLL DOWN FOR ARTICLE

Full terms and conditions of use: <http://www.informaworld.com/terms-and-conditions-of-access.pdf>

This article may be used for research, teaching and private study purposes. Any substantial or systematic reproduction, re-distribution, re-selling, loan or sub-licensing, systematic supply or distribution in any form to anyone is expressly forbidden.

The publisher does not give any warranty express or implied or make any representation that the contents will be complete or accurate or up to date. The accuracy of any instructions, formulae and drug doses should be independently verified with primary sources. The publisher shall not be liable for any loss, actions, claims, proceedings, demand or costs or damages whatsoever or howsoever caused arising directly or indirectly in connection with or arising out of the use of this material.

Modeling and Simulation of an Adiabatic Adsorber

P. S. K. CHOI,* L. T. FAN, and H. H. HSU†

DEPARTMENT OF CHEMICAL ENGINEERING
KANSAS STATE UNIVERSITY
MANHATTAN, KANSAS 66506

Abstract

An adiabatic fixed bed adsorber is modeled and simulated, and the effects of various parameters on its performance are investigated. The results of this study give an insight into the operating characteristics of the adsorption unit and should be useful in planning laboratory and field experiments and for interpreting the results of such experiments.

INTRODUCTION

A packed bed adsorption unit appears to be one of the most practical separation devices for gas purification, solvent recovery, product enrichment, air pollution control, and other similar processes. The performance of an adsorber is influenced by the chemical, physical, and thermodynamic properties of the adsorbent and adsorbate (1, 2). These properties include chemical constituents, extent of surface area, pore size distribution, size and shape of the adsorbate, and transport properties and equilibrium concentration of the adsorbent, all which are, in turn, functions of the operating temperature and pressure.

The flow pattern of the gas in a fixed bed adsorber also affects its performance significantly. Although the flow pattern in the fixed bed adsorber is very difficult to describe mathematically with accuracy, it can

*P. S. K. Choi is presently at the Battelle Memorial Institute, Columbus, Ohio.

†H. H. Hsu is presently at the Esso Production Research Company, Houston, Texas.

be approximated by either the plug flow model or the dispersion model (3). The plug flow model is valid if the adsorber bed is relatively deep and the movement of the adsorbate is predominated by the convective motion. The actual flow pattern of a gas through a fixed adsorption bed can deviate appreciably from that represented by the plug flow. Axial dispersion of the adsorbate can be caused by the turbulence, influence of the velocity profile, molecular diffusion, and convective mixing due to temperature differences. Therefore, the dispersion model is more realistic than the plug flow model to simulate the flow through a fixed bed, especially for a shallow bed.

In general, an adsorption process is accompanied by heat generation. The heat released in the process can be significant; it raises the temperature of the bed, and a rise in temperature affects the adsorption rate.

In the design and operation of an adsorption bed, it is necessary to predict the dynamic behavior of the bed, which is difficult since it is influenced by many factors. In this study the adiabatic adsorption process taking place in a fixed bed of adsorbent is mathematically modeled and numerically simulated. The effects of various design parameters, such as the Peclet number, external mass transfer coefficient, and the adsorbent capacity, are examined for the dynamic changes in the adsorbate concentration and temperature in both gaseous and solid phases of the bed.

MODEL EQUATIONS AND NUMERICAL SOLUTION

The assumptions made in deriving the model equations for the packed adsorber under consideration are that

- (a) An adsorption process taking place in a fixed bed is adiabatic.
- (b) The mass and heat transfers between gas and adsorbent phases are external transfer rate controlling.
- (c) The equilibrium isotherm between the two phases is of the Langmuir type (1, 2).
- (d) Parameters, such as heat and mass transfer coefficients, porosity of bed, adsorbent density, specific surface area, specific heats of gas and adsorbent, and heat conductivity of adsorbent, do not change with operating conditions.
- (e) No dispersion of the gaseous components occurs in the entrance and exit sections adjacent to the bed.

Mass and heat balances over a control volume of the bed lead to the

following partial differential equations:

$$H_g \frac{\partial c}{\partial t} = \Phi \rho_g E_1 \frac{\partial^2 c}{\partial z^2} - G \frac{\partial c}{\partial z} - R_a \quad (1)$$

$$H_s \frac{\partial q}{\partial t} = R_a \quad (2)$$

$$H_g c_g \frac{\partial T_g}{\partial t} = \Phi E_2 \frac{\partial^2 T_g}{\partial z^2} - G c_g \frac{\partial T_g}{\partial z} - h a (T_g - T_a) \quad (3)$$

$$H_s c_s \frac{\partial T_a}{\partial t} = (1 - \Phi) E_3 \frac{\partial^2 T_g}{\partial z^2} + h a (T_g - T_a) + (\Delta H_a) R_a \quad (4)$$

The initial and boundary conditions are, when $t = 0$:

$$c = 0 \quad (5)$$

$$q = 0 \quad (6)$$

$$T_g = T_0 \quad (7)$$

$$T_a = T_0 \quad (8)$$

at $z = 0$

$$G(c)|_{z=0^+} = Gc_f + \Phi \rho_g E_1 \left(\frac{\partial c}{\partial z} \right) \Big|_{z=0^+} \quad (9)$$

$$Gc_g(T_g)|_{z=0^+} = Gc_g T_0 + \Phi E_2 \left(\frac{\partial T_g}{\partial z} \right) \Big|_{z=0^+} \quad (10)$$

$$\frac{\partial T_a}{\partial z} = 0 \quad (11)$$

at $z = L$

$$\frac{\partial c}{\partial z} = 0 \quad (12)$$

$$\frac{\partial T_g}{\partial z} = 0 \quad (13)$$

$$\frac{\partial T_a}{\partial z} = 0 \quad (14)$$

The adsorption rate, R_a , for the external mass transfer control mechanism can be written as

$$R_a = k_e a \rho_g (c - c^*) \quad (15)$$

where c^* is the gas phase equilibrium concentration which can be expressed by a Langmuir-type isotherm

$$q = \frac{q_m b c^*}{1 + b c^*} \quad (16)$$

where

$$b = \frac{A_1 \exp(A_2/T_a)}{T_a^{\frac{1}{2}}} \quad (17)$$

Let

$$\begin{aligned} X &= c/c_f \\ Y &= q/q_m \\ U &= T_g/T_0 \\ V &= T_a/T_0 \\ \lambda &= z/L \\ \tau &= tG/LH_g \\ Pe_m &= GL/\Phi \rho_g E_1 \\ Pe_h &= \frac{GL}{\Phi \rho_g (E_2/\rho_g c_g)} = \frac{GL}{\Phi \rho_g E_2'} \quad \left(E_2' = \frac{E_2}{\rho_g c_g} \right) \\ K_e &= k_e a \rho_g L/G \\ H &= h a L/G c_g \\ K &= (1 - \Phi) E_3 H_g / GL H_s \\ \alpha &= H_g c_f / H_s q_m \\ \beta &= H_g c_g / H_s c_s \\ \gamma &= (\Delta H_a) H_g c_f / c_s H_s T_0 \end{aligned} \quad (18)$$

Then Eqs. (1) through (16) can be transformed into

$$\frac{\partial X}{\partial \tau} = \frac{1}{Pe_m} \frac{\partial^2 X}{\partial \lambda^2} - \frac{\partial X}{\partial \lambda} - K_e (X - X^*) \quad (19)$$

$$\frac{\partial Y}{\partial \tau} = \alpha K_e (X - X^*) \quad (20)$$

$$\frac{\partial U}{\partial \tau} = \frac{1}{\text{Pe}_h} \frac{\partial^2 U}{\partial \lambda^2} - \frac{\partial U}{\partial \lambda} - H(U - V) \quad (21)$$

$$\frac{\partial V}{\partial \tau} = \frac{K \partial^2 V}{\partial \lambda^2} + \beta H(U - V) + \gamma K_e (X - X^*) \quad (22)$$

$$Y = \frac{BX^*}{1 + BX^*} \quad (23)$$

The corresponding initial and boundary conditions are, when $\tau = 0$:

$$X = 0 \quad (24)$$

$$Y = 0 \quad (25)$$

$$U = 1 \quad (26)$$

$$V = 1 \quad (27)$$

at $\lambda = 0$

$$(X)|_{\lambda=0^+} = 1 + \frac{1}{\text{Pe}_m} \left(\frac{\partial X}{\partial \lambda} \right) \Big|_{\lambda=0^+} \quad (28)$$

$$(U)|_{\lambda=0^+} = 1 + \frac{1}{\text{Pe}_h} \left(\frac{\partial U}{\partial \lambda} \right) \Big|_{\lambda=0^+} \quad (29)$$

$$\partial V / \partial \lambda = 0 \quad (30)$$

at $\lambda = 1$

$$\partial X / \partial \lambda = 0 \quad (31)$$

$$\partial U / \partial \lambda = 0 \quad (32)$$

$$\partial V / \partial \lambda = 0 \quad (33)$$

where

$$B = \frac{A_1' \exp(A_2'/V)}{V^{\frac{1}{2}}} \quad (34)$$

If the mass dispersion coefficient, E_1 , is assumed to be equal to the thermal dispersion coefficient, E_2' (or $E_2/\rho_g c_g$), then

$$\text{Pe}_m = \text{Pe}_h = \text{Pe} \quad (35)$$

It would be very difficult, if not impossible, to obtain analytical solutions for the simultaneous partial differential equations (Eqs. 19 through 23)

subject to the initial and boundary conditions (Eqs. 24 through 33). Computer-aided numerical methods can be employed for solution. These methods include the finite difference method, method of characteristics, and collocation method. Among these, the implicit finite difference method, specifically the Crank-Nicolson method, is employed in this study. The method involves less stringent stability and convergence restrictions than the explicit finite difference method and requires less computing time than the method of characteristics. In addition, this method is known to be particularly powerful for the parabolic partial differential equations encountered in this study.

In employing the Crank-Nicolson method, each partial differential equation is rewritten as a set of simultaneous algebraic equations. Since a detailed description of the method is available elsewhere (4, 5), the derivation of the simultaneous algebraic equations and the solution thereof by using the Thomas algorithm are not given here.

RESULTS AND DISCUSSIONS

The Langmuir-type isotherm given in Eq. (23) is plotted in Fig. 1 for $A_1' = 1.35 \times 10^{-6}$ and $A_2' = 15.04$. This isotherm is employed throughout this study. Figure 2 shows the adsorbate concentration distributions in a packed bed adsorber for different values of operating time. The adsorbate concentrations in the gaseous and solid phases of the bed are initially zero. When adsorbate laden gas is introduced, the adsorbate penetrates into the void in the bed by convection and diffusion, and simultaneously the adsorption process takes place between the adsorbate in the void and the surface of the adsorbent. This results in the gas phase adsorbate concentration profile decreasing in the axial direction of flow. As time increases, the adsorbent surface is gradually saturated and the adsorbate concentration in the gaseous phase becomes higher. As τ approaches infinity, the adsorbent is completely saturated and the exit concentration becomes the same as the inlet concentration. At the same time, the adsorbate concentration on the adsorbent assumes the equilibrium value with respect to the inlet concentration at the inlet temperature. The effect of dispersion results in the adsorbate concentration drop at the entrance of the bed as shown in Fig. 2. The magnitude of the concentration drop depends on the intensity of dispersion expressed in terms of the Peclet number and the magnitude of the concentration gradient.

Figure 3 shows the temperature distributions of the gas and solid

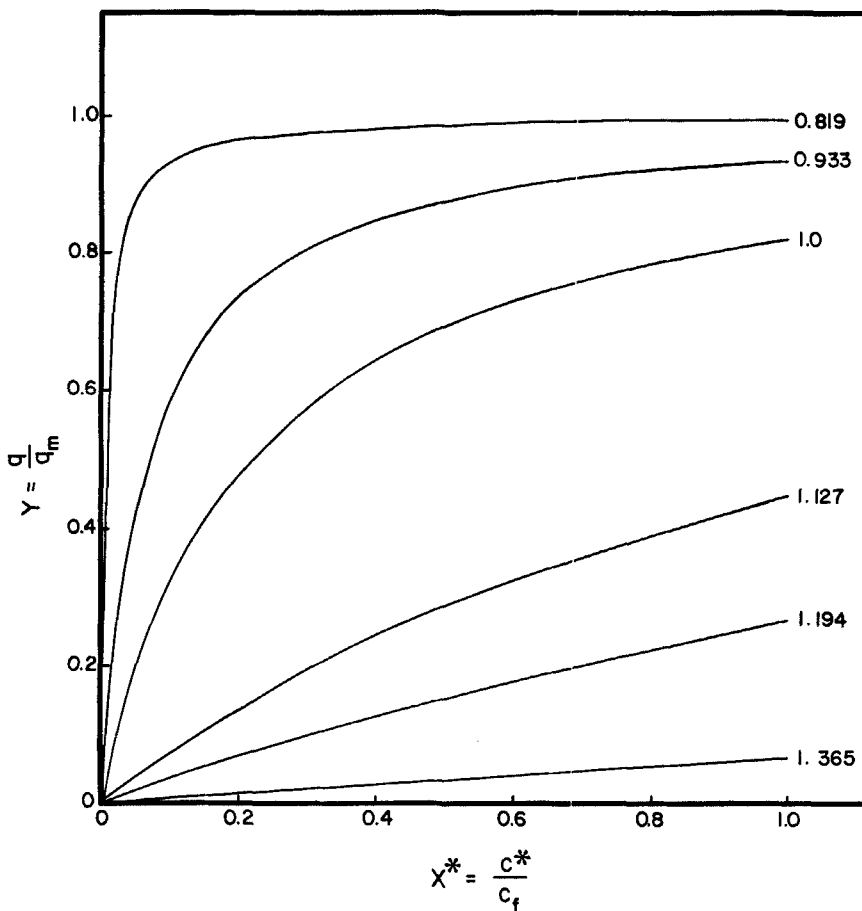


FIG. 1. Adsorption isotherm plotted according to a Langmuir-type isotherm, Eq. (23) (parameter, V).

phases. The temperatures are assumed to be initially identical with the room temperature (or the inlet gas temperature). Heat released from the adsorption process raises the adsorbent temperature as well as the gas phase temperature. The maximum gas and solid phase temperatures occur initially at the entrance of the bed and gradually move in the direction of gas flow as the zone of maximum adsorption rate moves in the same direction. The maximum gas temperature always appears at a distance farther down the bed than the maximum adsorbent temperature due to

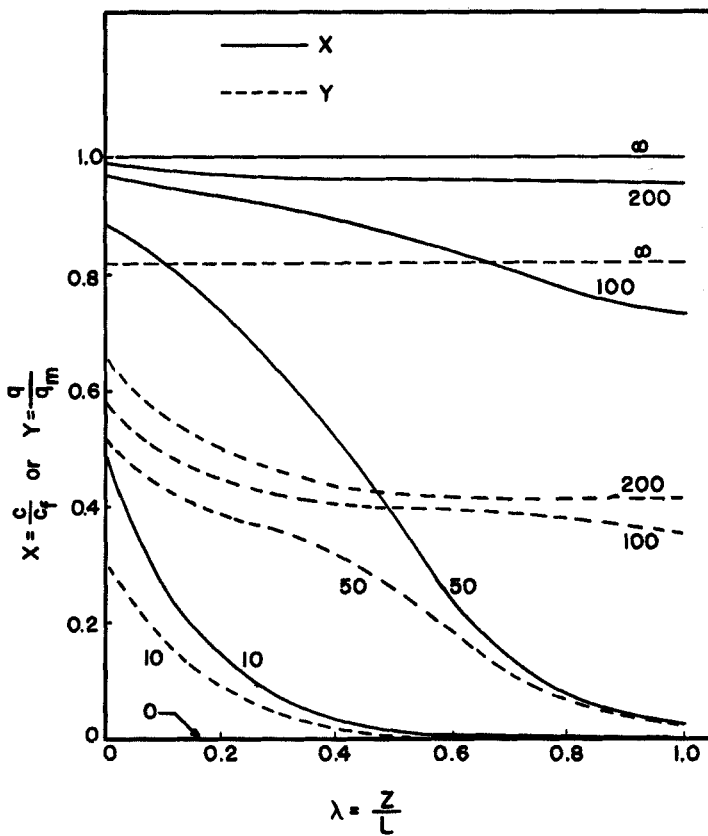


FIG. 2. Adsorbate concentration distribution in a packed bed adsorber ($Pe = 5$, $K_e = 20$, $H = 100$, $\alpha = 0.005$, $\beta = 0.001$, $\gamma = 0.002$; parameter, τ).

the convection of heat in the gas phase in the direction of flow. The effect of dispersion on the jump in the gas temperature at the entrance can also be observed in Fig. 3. The temperature gradient in the gas phase generated by the heat of adsorption causes heat to be dispersed in the directions along and opposite to the gas flow. Since no heat is transported out of the bed into the entrance section, heat dispersed in the direction opposite to the gas flow is reflected into the bed at the entrance. This renders the gas phase temperature at the entrance of the bed to be higher than the incoming gas temperature. This phenomenon is especially pronounced at the onset of the operation. When time τ approaches infinity, the bed tempera-

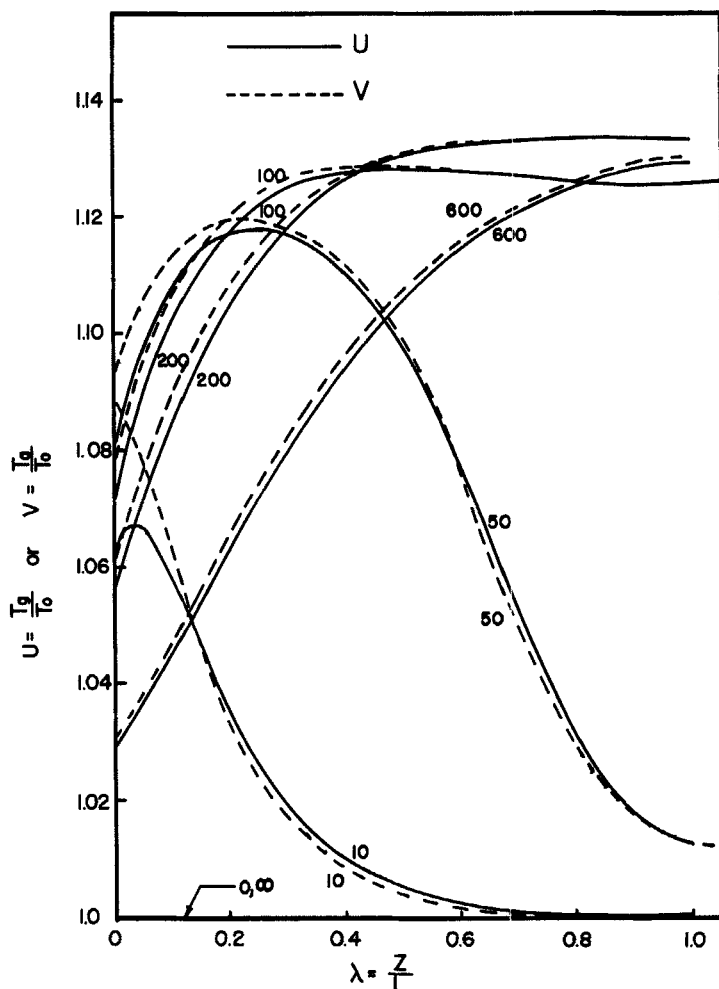


FIG. 3. Temperature distribution in a packed bed adsorber ($Pe = 5$, $K_e = 20$, $H = 100$, $\alpha = 0.005$, $\beta = 0.001$, $\gamma = 0.002$; parameter, τ).

ture becomes the same as the incoming gas temperature because the rate of heat generation decreases with an increase in the degree of saturation of the adsorbate on the adsorbent, and the heat generated is rapidly removed by the gas flowing through the bed.

The effect of dispersion as characterized by the Peclet number on the

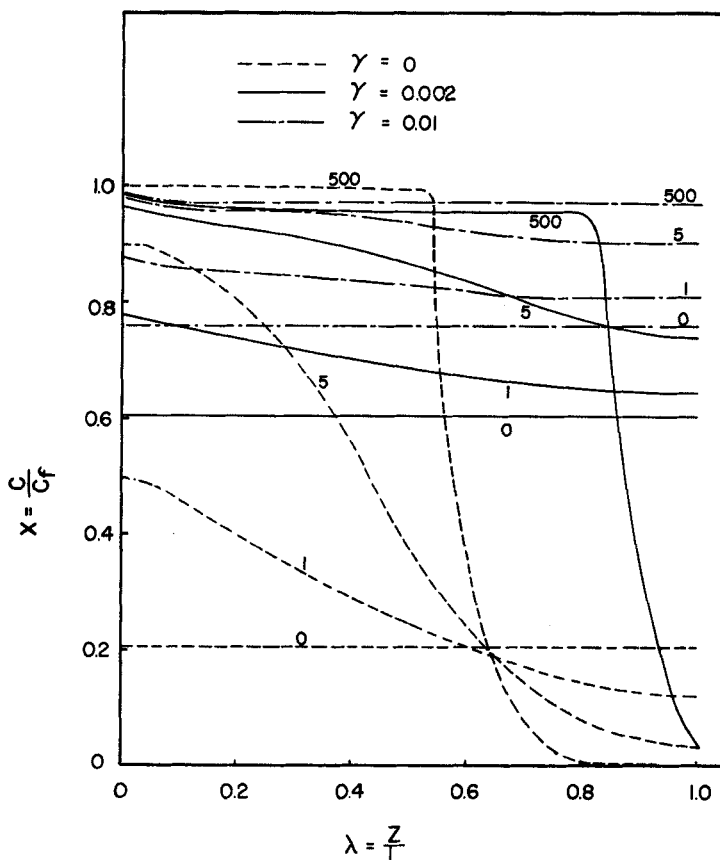


FIG. 4. Effect of Peclet number on the gas phase adsorbate concentration distribution in a packed bed adsorber at $\tau = 100$ ($K_e = 20$, $H = 100$, $\alpha = 0.005$, $\beta = 0.001$; parameter, Pe).

concentration in the gas phase of the bed at $\tau = 100$ for different values of the heat of adsorption is shown in Fig. 4, and that in the solid phase in Fig. 5. As expected, these figures show that the adsorbate concentrations are uniform throughout the bed when $Pe = 0$ (complete mixing). For large values of Pe , e.g., $Pe = 500$, the flow behavior is essentially that of the plug flow. For intermediate values of Pe , namely for a finite degree of dispersion, the adsorbate concentration profiles fall between the profiles for complete mixing and that for plug flow. The effect of heat of adsorption is also clearly shown in the figures. Figure 4 shows that, for the same

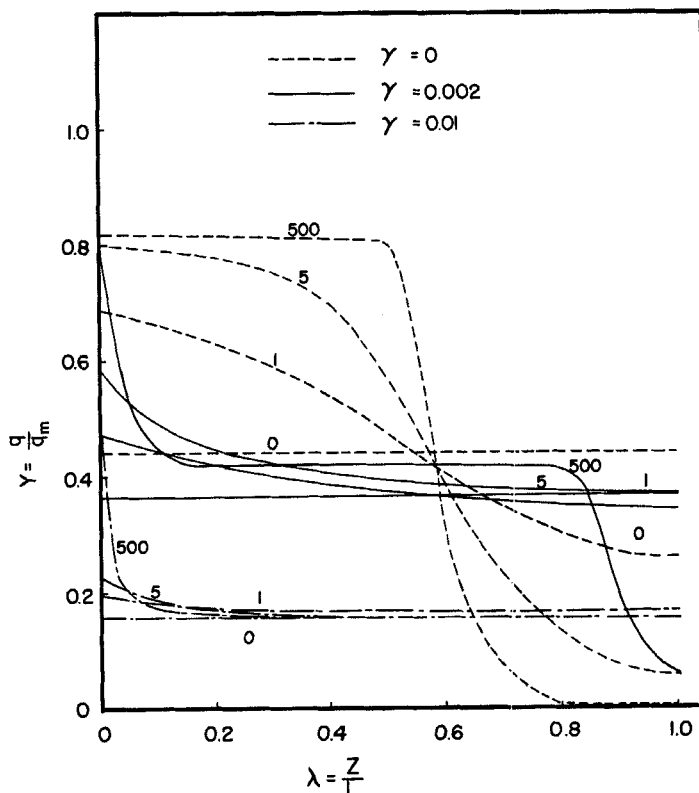


FIG. 5. Effect of Peclet number on the solid phase adsorbate concentration distribution in a packed bed adsorber at $\tau = 100$ ($K_e = 20$, $H = 100$, $\alpha = 0.005$, $\beta = 0.001$; parameter, Pe).

value of the Peclet number, the average adsorbate concentration in the gas phase is lower for the isothermal case ($\gamma = 0$) than for the non-isothermal case ($\gamma > 0$). Conversely, Fig. 5 shows that the average adsorbate concentration in the solid phase is higher for the isothermal case than for the nonisothermal case. In other words, the adsorption process proceeds faster in an isothermal bed than in a nonisothermal bed. This is because the heat generated from the adsorption process in a nonisothermal bed raises the solid phase temperature, thus resulting in a smaller driving force for adsorbate transfer.

The effect of dispersion on the temperature distributions in the gas and

solid phases in the bed is shown in Fig. 6. For $Pe = 0$ (complete mixing), the temperature profiles are flat across the bed as expected. The solid phase temperature is higher than the gas phase temperature because heat is generated in the solid phase, raising the solid phase temperature first, and then is transported to the gas phase. When the Peclet number increases, the temperatures in both phases increase sharply near the entrance and

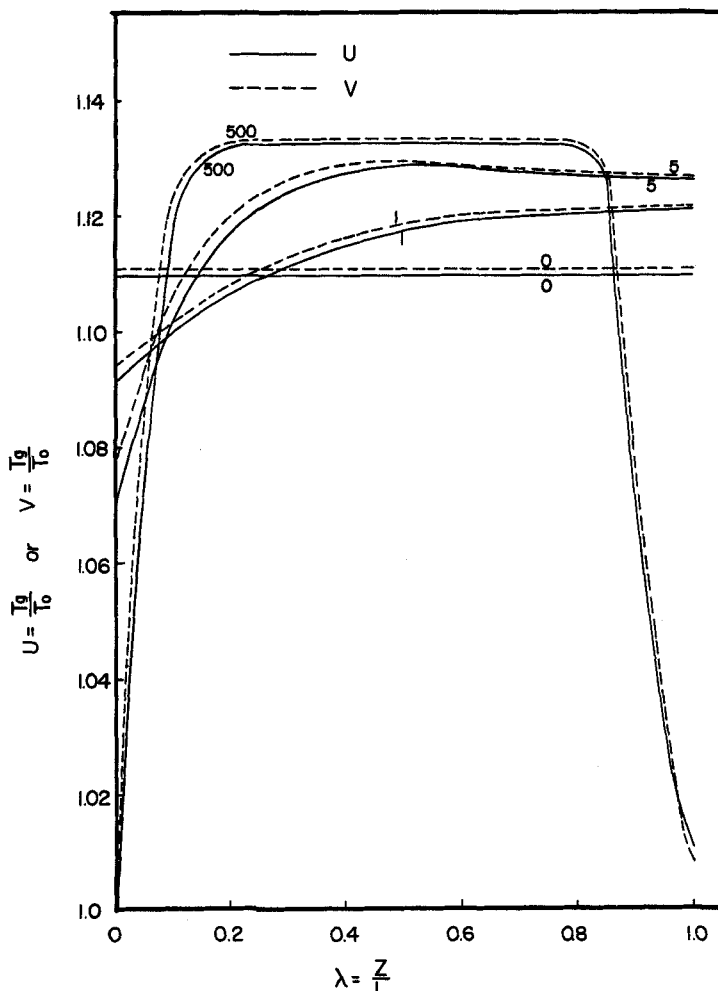


FIG. 6. Effect of Peclet number on the temperature distribution in a packed bed adsorber at $\tau = 100$ ($K_e = 20$, $H = 100$, $\alpha = 0.005$, $\beta = 0.001$, $\gamma = 0.002$; parameter, Pe).

then level off. For large values of the Peclet number, e.g., $Pe = 500$, the temperatures drop sharply near the exit. This is reasonable since little adsorption has occurred near the exit as reflected by Figs. 4 and 5.

Figure 7 shows the effect of dispersion on the breakthrough of the incoming gas. For small values of the Peclet number, the dispersion of the gas is so intensive that the adsorbate is almost uniformly distributed in the bed. The adsorbate concentration in the gas phase near the exit is almost the same as that near the entrance. Therefore, the adsorbate breaks through the bed fairly rapidly. For large values of the Peclet number, however, the gas is not well dispersed. The bed is saturated with the adsorbate progressively from the entrance toward the exit. The adsorbate

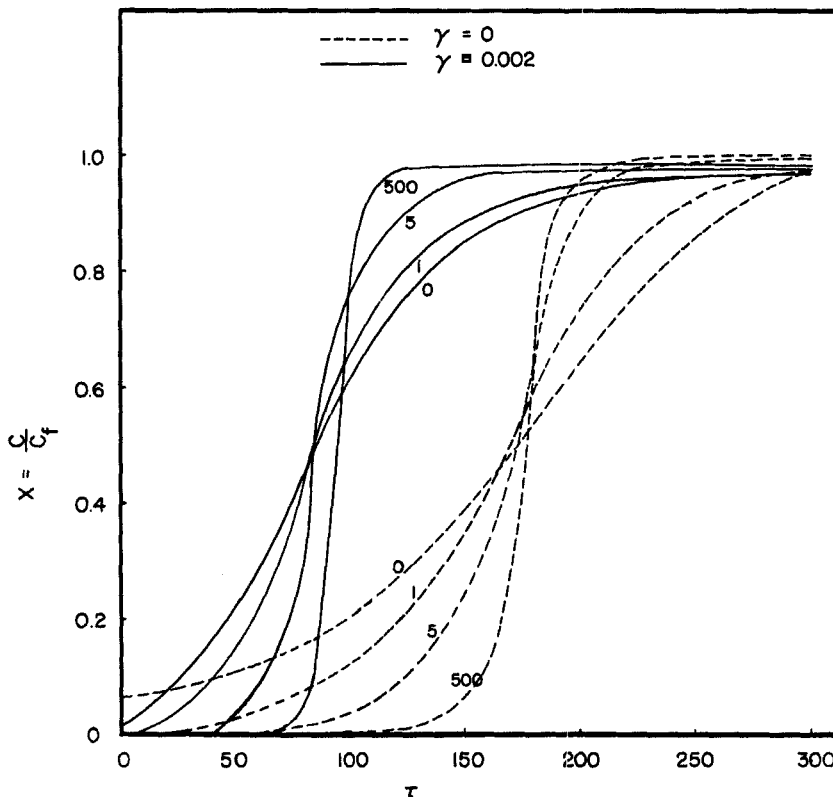


FIG. 7. Effect of Peclet number on the exit adsorbate concentration change in a packed bed adsorber ($K_e = 20$, $H = 100$, $\alpha = 0.005$, $\beta = 0.001$; parameter, Pe).

does not move downstream either by convection or by diffusion unless it finishes saturating the portion of the bed it has contacted. Thus a moving front is formed which separates the bed into two distinct portions: one with complete contamination and the other with no contamination. In this manner the breakthrough occurs relatively late and sharply. It is worth noting that, for the same value of the Peclet number, the breakthrough occurs earlier for the nonisothermal process than for the isothermal process.

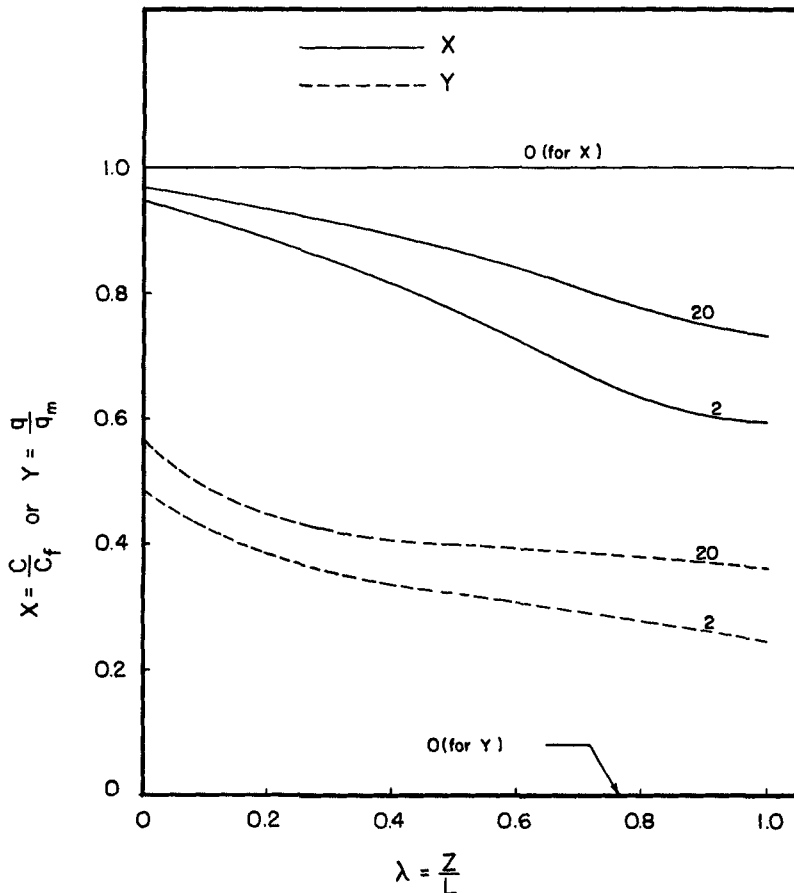


FIG. 8. Effect of K_e on the adsorbate concentration distribution in a packed bed adsorber at $\tau = 100$ ($Pe = 5$, $H = 100$, $\alpha = 0.005$, $\beta = 0.001$, $\gamma = 0.002$; parameter, K_e).

Figure 8 shows the effect of dimensionless external mass transfer coefficient, K_e , on the adsorbate concentration distribution. For $K_e = 0$, no adsorption takes place in the bed, and therefore the void space of the bed is completely filled with the incoming gas and the adsorbent remains uncontaminated. For K_e values other than zero, the concentrations of both the gas and solid phases in the bed are higher for large values of K_e than for small values of K_e since the bed is saturated more rapidly for large value of K_e .

Figure 9 shows the effect of α , the inverse of the adsorption capacity of

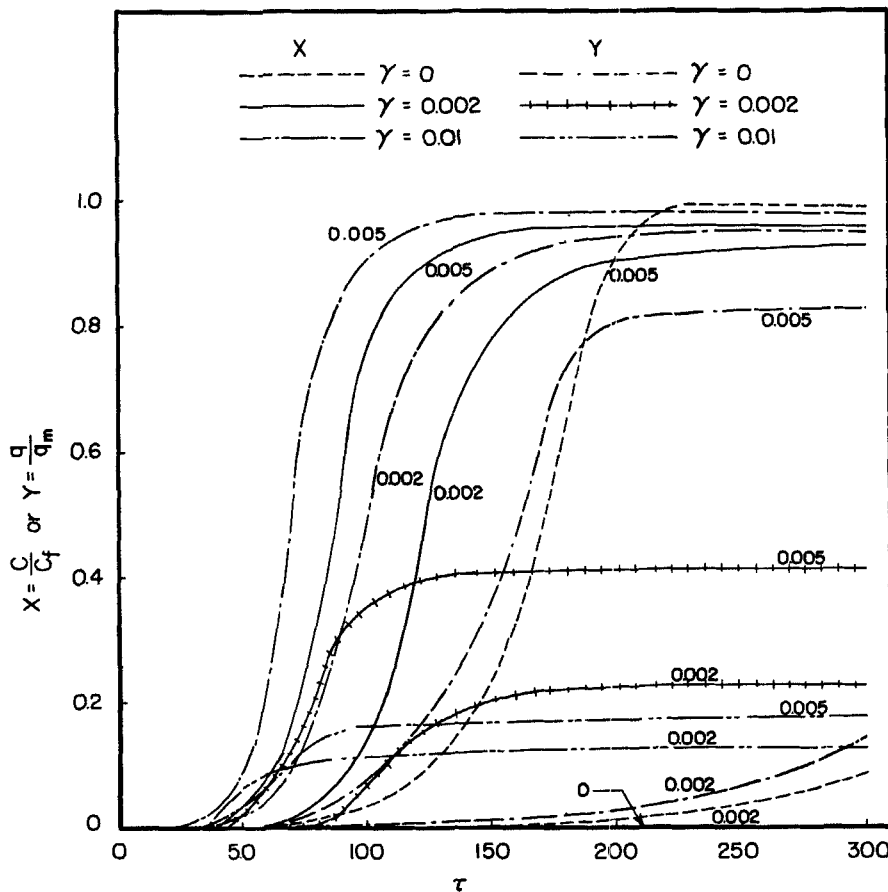


FIG. 9. Effect of α on the exit adsorbate concentration change in a packed bed adsorber ($Pe = 5$, $K_e = 20$, $H = 100$, $\beta = 0.001$; parameter, α).

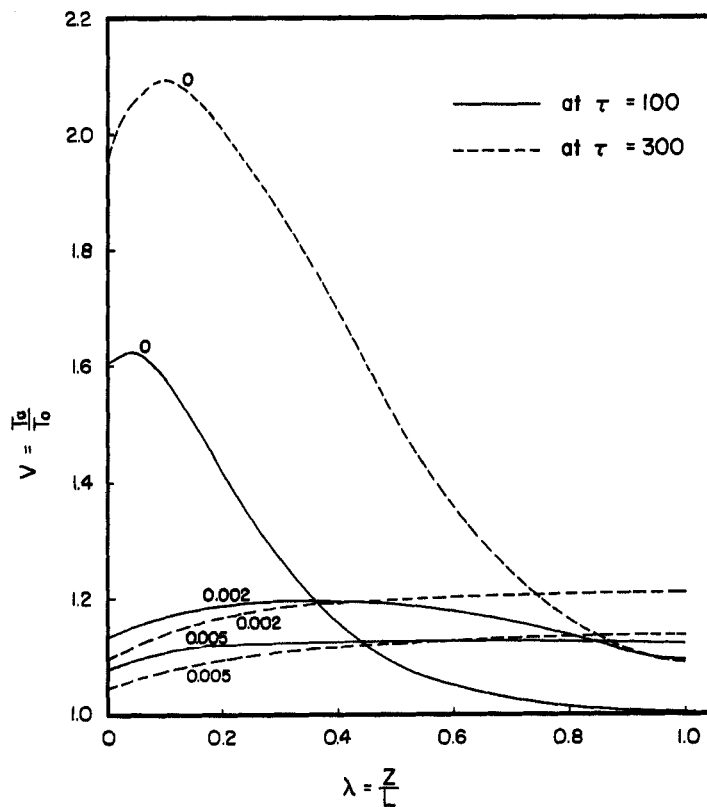


FIG. 10. Effect of α on the solid phase temperature distribution in a packed bed adsorber ($Pe = 5$, $K_e = 20$, $H = 100$, $\beta = 0.001$, $\gamma = 0.002$; parameter, α).

the bed, on the transient adsorbate concentration at the exit for three different values of the heat of adsorption. For $\alpha = 0$, or $1/\alpha \rightarrow \infty$, the bed has infinite adsorption capacity and is never saturated. For large values of α , or small values of $1/\alpha$, the adsorption capacity is small; therefore the bed is rapidly saturated. The effect of α on the solid phase temperature distribution in the bed is shown in Fig. 10. For small values of α , more adsorbate can be adsorbed and more heat is generated in the bed. This may result in very high temperatures in the bed. In particular, for $\alpha = 0$, the bed temperature may rise continuously with time until heat generation is equal to heat removal by gas flow. In this case the adsorber

temperature may rise to a very high level, and consequently the stability problem becomes serious.

A further insight into the operation of an adsorber unit can be gained through evaluation of cumulative adsorption efficiency. A macroscopic adsorbate balance over the total volume of the bed gives

$$c_f G t = \int_0^t c_e G \, dt + \int_0^L c H_g \, dz + \int_0^L q H_s \, dz \quad (36)$$

By introducing dimensionless quantities in Eq. (18), Eq. (36) can be rewritten as

$$\tau = \int_0^\tau X_e \, d\tau + \int_0^1 X \, d\lambda + \frac{1}{\alpha} \int_0^1 Y \, d\lambda \quad \text{if } \alpha \neq 0$$

or

$$\tau = \int_0^\tau X_e \, d\tau + \int_0^1 X \, d\lambda \quad \text{if } \alpha = 0$$

Thus the cumulative adsorption efficiency can be defined as

$$\eta_a = 1 - \frac{1}{\tau} \int_0^\tau X_e \, d\tau \quad (38)$$

or

$$\begin{aligned} \eta_a &= \frac{1}{\tau} \left\{ \int_0^1 X \, d\lambda + \frac{1}{\alpha} \int_0^1 Y \, d\lambda \right\} \quad \text{if } \alpha \neq 0 \\ &= \frac{1}{\tau} \int_0^1 X \, d\lambda \quad \text{if } \alpha = 0 \end{aligned} \quad (39)$$

Note that the adsorption efficiency changes with time and can be obtained by integrating either Eq. (38) or (39) numerically.

Figure 11 shows the effect of axial dispersion characterized by the Peclet number on the cumulative adsorption efficiency. The adsorption efficiency is generally increased when dispersion is less significant and vice versa. In all cases the cumulative adsorption efficiency decreases as time increases because the bed becomes saturated gradually. The effect of heat of adsorption, γ , is also shown in the figure. It is readily seen that the cumulative adsorption efficiencies are lower for the nonisothermal cases ($\gamma > 0$) than for the isothermal case ($\gamma = 0$).

The effect of the inverse adsorption capacity α on the cumulative

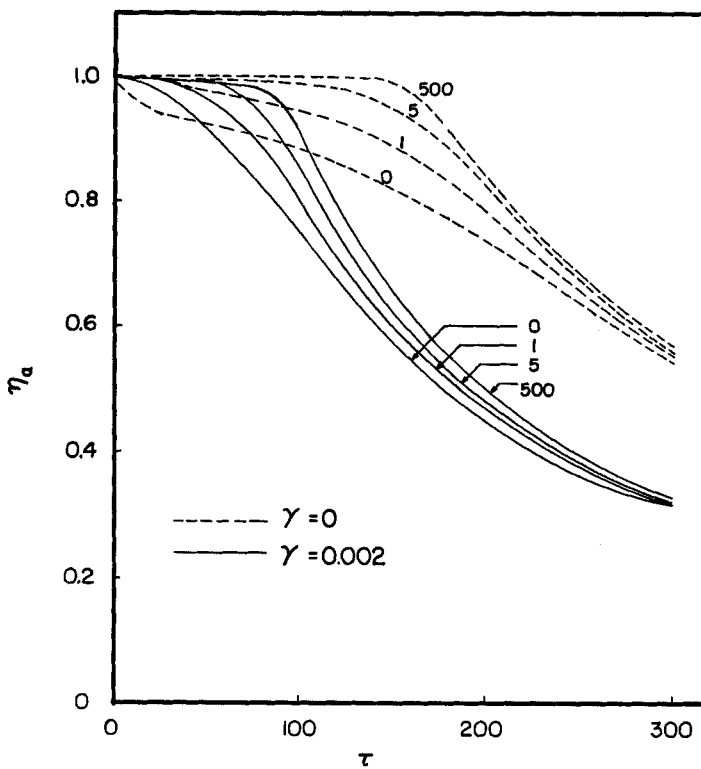


FIG. 11. Effect of Peclet number on the cumulative adsorbate removal efficiency ($K_e = 20$, $H = 100$, $\alpha = 0.005$, $\beta = 0.001$; parameter, Pe).

adsorption efficiency at different values of γ is shown in Fig. 12. When α is small the adsorption capacity of the bed is large, resulting in slow saturation of the bed and, consequently, in a high cumulative adsorption efficiency.

CONCLUDING REMARKS

A mathematical simulation study of the processes taking place in an adiabatic adsorption bed is carried out, and the combined effect of dispersion and heat of adsorption on the operating characteristics of the adsorption unit is determined. The results of this study are useful for prediction of the behavior of an adiabatic adsorption bed, for designing and operating

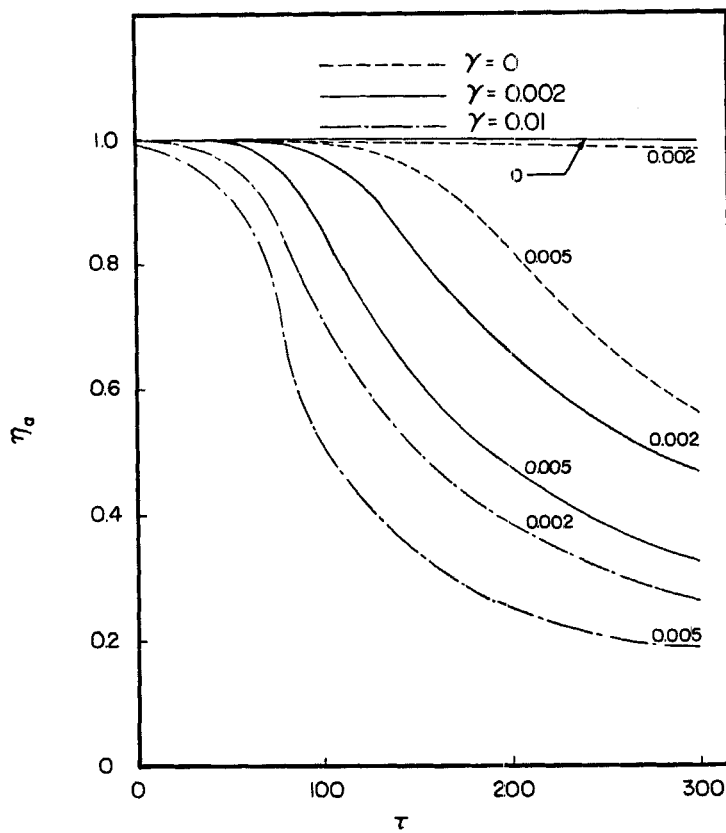


FIG. 12. Effect of α on the cumulative adsorbate removal efficiency ($Pe = 5$, $K_e = 20$, $H = 100$, $\beta = 0.001$; parameter, α).

it, for planning laboratory and field experiments with it, and for interpreting the results of such experiments.

SYMBOLS

a	available external surface area per unit volume of bed, cm^2/cm^3
A_1	constant, $^{\circ}\text{K}^{1/2}$
A_1'	constant, $c_f A_1/T_0^{1/2}$
A_2	constant, $^{\circ}\text{K}$
A_2'	constant, A_2/T_0

<i>b</i>	adsorption coefficient expressed in Eq. (17)
<i>B</i>	constant expressed in Eq. (34)
<i>c</i>	adsorbate concentration in gas phase, g of adsorbate/g of adsorbate free gas
<i>c</i> *	equilibrium concentration, g of adsorbate/g of adsorbate free gas
<i>c_f</i>	feed concentration, g of adsorbate/g of adsorbate free gas
<i>c_g</i>	specific heat of gas, cal/°K-g
<i>c_s</i>	specific heat of solid adsorbent, cal/°K-g
<i>E₁</i>	axial mass dispersion coefficient in the gas phase, cm ² /sec
<i>E₂</i>	axial dispersive conductivity of the gas phase, cal/sec, °K-cm
<i>E₂'</i>	axial thermal dispersion coefficient in the gas phase, cm ² /sec
<i>E₃</i>	thermal conductivity of solid, cal/sec-°K-cm
<i>G</i>	superficial mass flow rate of fluid per unit cross-sectional area, g of gas/sec-cm ²
<i>h</i>	heat transfer coefficient between gas and adsorbent, cal/°K-cm ² -sec
<i>H</i>	dimensionless heat transfer coefficient, hAL/Gc_g
<i>H_g</i>	gas phase hold-up, i.e., mass of gas per unit volume of bed, g of gas/cm ³ of bed
<i>H_s</i>	solid phase hold-up, i.e., mass of adsorbent per unit volume of bed, g of adsorbent/cm ³ of bed
ΔH_a	average heat of adsorption, cal/g
<i>k_e</i>	external mass transfer coefficient based on external surface of particle and concentration driving force, cm/sec
<i>K</i>	dimensionless adsorbent heat conductivity, $(1 - \Phi)E_3H_g/GLH_s$
<i>K_e</i>	dimensionless mass transfer coefficient, $k_e\alpha\rho_g L/G$
<i>L</i>	depth of adsorption bed, cm
Pe	Peclet number
Pe _h	Peclet number for heat transfer, $GL/\Phi\rho_g E_2'$
Pe _m	Peclet number for mass transfer, $GL/\Phi\rho_g E_1$
<i>q</i>	amount of adsorbate adsorbed per unit mass of adsorbent, g of adsorbate/g of adsorbent
<i>q_m</i>	maximum amount of adsorbate which can be adsorbed per unit mass of adsorbent, g of adsorbate/g of adsorbent
<i>R_a</i>	overall rate of adsorption per unit volume of bed, g/sec-cm ³
<i>t</i>	time, sec
<i>T_a</i>	adsorbent temperature, °K
<i>T_g</i>	gas temperature, °K
<i>T₀</i>	temperature at the inlet of the bed, °K
<i>U</i>	dimensionless gas temperature, T_g/T_0

V	dimensionless adsorbent temperature, T_a/T_0
X	dimensionless adsorbate concentration in gas phase, c/c_f
X^*	dimensionless adsorbate equilibrium concentration in gas phase, c^*/c_f
Y	dimensionless adsorbate concentration in solid phase, q/q_m
z	axial distance from entrance of bed, cm

Greek Letters

α	inverse of the adsorption capacity of the bed, $H_g c_f / H_s q_m$
β	ratio of heat capacity of gas phase to that of solid phase in the bed, $H_g c_g / H_s c_s$
γ	dimensionless heat of adsorption, $(\Delta H_a) H_g c_f / c_s H_s T_0$
η_a	cumulative adsorption efficiency
λ	dimensionless axial distance, z/L
ρ_g	density of gas, g/cm ³
τ	dimensionless time, tG/LH_g
Φ	void fraction of the bed

Acknowledgments

The authors wish to express their appreciation to the Environmental Protection Agency for financial support (Grant No. R800316), to the Kansas State University computer center for use of the IBM 360 computer, and also to Mr. K. B. Wang for his assistance.

REFERENCES

1. S. Brunauer, *The Adsorption of Gases and Vapors, Volume 1, Physical Adsorption*, Princeton University Press, Princeton, New Jersey, 1943.
2. D. M. Young and A. D. Crowell, *Physical Adsorption of Gases*, Butterworth, London, 1962.
3. C. Y. Wen and L. T. Fan, *Models for Flow Systems*, Gordon and Breach, New York, In Press.
4. L. Lapidus, *Digital Computation for Chemical Engineering*, McGraw-Hill, New York, 1962.
5. G. D. Smith, *Numerical Solution of Partial Differential Equations*, Oxford University Press, Oxford, 1965.

Received by editor January 27, 1975